SCEC Award 22037

NASA Collaborative Research: Three-dimensional displacement and strain rates from the integration of GNSS and InSAR for the Community Geodetic Model

Final Technical Report

Michael Floyd[1] and Katia Tymofyeyeva[2]
[1]*Massachusetts Institute of Technology*, [2]*NASA Jet Propulsion Laboratory*

Summary

We present two results from contributions to the Community Geodetic Model (CGM), which were identified during this award as being important initial steps to combine InSAR with GNSS products (time series and velocities) ultimately and successfully. We have quantified uncertainties for both InSAR time series and InSAR velocities, based on the variance of contributing solutions and time series analysis similar to standard approaches for GNSS, respectively. We have also shown that a plate rotation beneath the SAR satellite orbits, nominally in the International Terrestrial Reference Frame 2014 (ITRF2014), produces a measureable velocity gradient, which must be accounted for when producing InSAR time series and velocities over a significant portion of the Earth's surface. The latter has also been demonstrated, and published, by Stephenson et al. (2022). Finally, we have both continued to lead and coordinate the Working Groups of the CGM, with PI Tymofyeyeva chairing online meetings of the CGM (InSAR) Working Group once every two weeks and PI Floyd overseeing the CGM as a whole, in particular the GNSS component. Much of the work and progress reported here was, and continues to be, informed and guided by those regular meetings, as new barriers are identified and solutions proposed and tested.

Uncertainties for InSAR time series and velocities

During discussions with the CGM (InSAR) Working Group and through our own efforts to combine the CGM's GNSS component with the newly developed InSAR products, it became obvious quickly that further progress could not be made without the assignment of realistic uncertainties for both the InSAR time series and velocities. InSAR has commonly been used in the past to study large deformations, such as earthquakes and volcanic eruptions, where the uncertainties inherent in the method tend to be insignificant compared to the deformation, implicitly having a very large signal-to-noise ratio. This is not the case when using InSAR to study slow deformation signals, such as those associated with interseismic deformation of the plate boundary across Southern California.

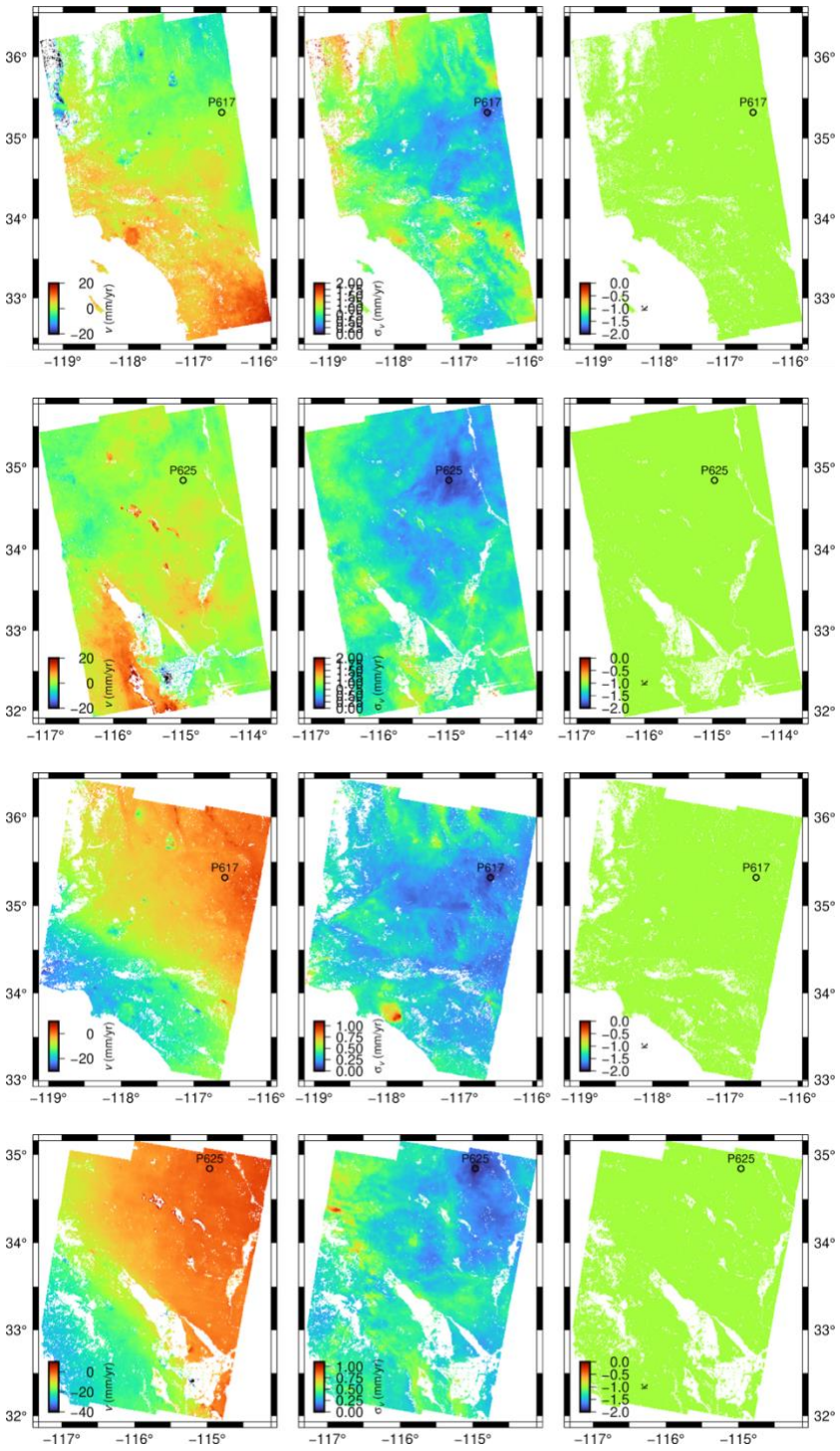

Figure 1 *Demonstration of InSAR uncertainties when considering the effect of temporally correlated noise, as is standard practice when analysing GNSS time series, for ascending track 64 (top row), ascending track 166 (second row), descending track 71 (third row) and descending track 173 (bottom row), not including seasonal terms. A power law noise model is assumed, with a freely estimated exponent parameter, using Hector (Bos et al., 2013) here. Velcocities (left), associated uncertainties (middle) and the power law exponent (right) are estimated directly from the InSAR time series.*

For the CGM InSAR time series, a simple standard deviation is calculated and assigned to each data point, reflecting the formal variance of the several contributing solutions. For the velocities, it is standard practice when fitting GNSS time series to account for temporally correlated noise (e.g. Zhang et al., 1997; Williams, 2003), which in practice scales the formal uncertainty, assuming independent data points, by a factor of about two to five. We applied two common algorithms for GNSS time series analysis, "Hector" (Bos et al., 2003) and "FOGMEx" (Floyd and Herring, 2020), to the estimation of velocities and their uncertainties in this way from the CGM's InSAR time series, assuming a power law noise model with a free exponent parameter for Hector. These two approaches are generally designed to estimate results from daily time series, as is common for continuous GNSS products, but both are capable of similarly estimating using other sampling frequencies. Hector requires regularly spaced data points to take advantage of implicit assumptions that speed up its calculations, which for the most part is true of the CGM InSAR time series, with a sampling period of nominally every 12 days and usually every six days with the repeat passes of the Sentinel-1 satellite. FOGMEx does not inherently require regularly spaced data but works best with a significant number of data points over a long time interval, which the CGM InSAR time series satisfies (about 90 acquisitions over 4.5 years from early 2015 to the Ridgecrest earthquakes, when the products tested here end).

Figure 1 shows the results from Hector, not including seasonal terms when fitting the time series for each pixel in each of the four currently used Sentinel-1 tracks over Southern California. The lowest uncertainties (near zero) correspond to the region around the reference pixel, annotated with a black circle in Figure 1, in each case. Including seasonal terms slightly reduces the uncertainties all around, because some of the power at the seasonal period is being explicitly fit rather than considered part of the "noise", but the pattern of relative uncertainties is much the same. Uncertainties are generally around 0.25-0.50 mm/yr over most of the region from the descending tracks, and about twice that from the ascending tracks. Relatively higher uncertainties are seen in areas of non-secular deformation, such as the Santa Ana aquifer, visible as an orange and red area in descending track 71 (middle of third row in Figure 1), where increased variability in the time series due to anthropogenic effects, which are correlated in time, should be quantified with higher uncertainties relative to a linear velocity fit.

The exponent of the power law estimated from all InSAR time series here is very close to −1 everywhere (right panels in Figure 1), approximating flicker noise. We are unsure of why this may be. Power law noise close to flicker noise is commonly displayed by GNSS time series but analyses of stations across any given region rarely show such spatial coherence, given local effects of monument foundation and stability. We suggest that the phenomena may be a result of the smoothing applied to generate the InSAR time series, depending on the algorithm chosen for each of the contributing solutions, or a consequence of the reduced sampling interval relative to the standard daily interval for which at least the Hector algorithm, which may mean that some of frequencies (periods) of the power spectrum may not be evaluated, reducing the ability of the algorithm to detect spatial variations from location to location. Nevertheless, we feel that this is a reasonable approximation of temporally correlated noise displayed by the InSAR time series and, as such, should be accounted for when fitting time series to estimate velocities and their associated uncertainties.

Other members of the CGM (InSAR) Working Group created their own implementations of this approach (e.g. K. Guns and X. Xu at UC San Diego and S. Sangha at NASA JPL), using the assumption of flicker noise to make assumptions that speed up the process of estimating velocities and their uncertainties over the spatially very dense InSAR. This work was presented at the 2022 SCEC Annual Meeting (Tymofyeyeva, Floyd, et al., 2022).

Effects of plate motion on InSAR displacements and velocities

Following the study and assignment of more realistic velocity uncertainties for the InSAR product, the CGM (InSAR) Working Group began to compare the InSAR and GNSS velocities more directly. K. Materna (USGS) noted that this comparison produced an apparent systematic offset of the InSAR velocities compared to the GNSS velocities projected into the InSAR line of sight (at least in bulk when visualized on a ratio plot such as the bottom two rows of Figure 2). The Working Group debated this, including the possibility that the GNSS and InSAR solutions were fundamentally offset from one another, perhaps due to some difference at the reference pixel, which led to a discussion about reference frames, albeit regarding the velocity gradient that would be induced across an InSAR scene rather than a velocity offset at the track's origin (reference pixel). We decided to test the effect of North America plate motion on the InSAR velocity solution, considering that the (now very accurate) Sentinel-1 orbit products with which the InSAR is processed are nominally in a no-net-rotation (ITRF2014) reference frame whereas the GNSS velocity solution is expressed relative to North America. Our hypothesis was that, although the reference pixel, which coincides with a GNSS station at this time, sets the origin of the InSAR reference frame for comparison to GNSS, there may be a (spatial) velocity gradient induced by the rotation of the North America plate beneath the nominal orbital reference frame, which might result in increasingly large discrepancies between the InSAR and GNSS away from the reference point.

We engaged in an experiment with other CGM (InSAR) Working Group members, Kang Wang (UC Berkeley) and Xioahua Xu (UC San Diego, now University of Science and Technology of China) to demonstrate and verify the expected InSAR signal when there is rigid-plate terrestrial motion beneath the implicit reference frame imposed by the orbit products used to generate the InSAR time series. Both K.W. and X.X. used a spherical Earth to calculate position vectors for the cross-product with the plate rotation rate vector, whereas we used the standard ellipsoidal Earth to calculate ours, e.g.:

$$\mathbf{v} = \boldsymbol{\omega} \times \mathbf{p}$$

where v is the plate rotation velocity at a site with position vector $\mathbf{p}$ and $\boldsymbol{\omega}$ is the rotation rate vector for the plate, e.g. relative to the no-net-rotation ITRF2014. We then convert the geocentric (X,Y,Z) coordinates from this equation to local geodetic (e,n,u):

$$\begin{pmatrix} v_e \\ v_n \\ v_u \end{pmatrix} = \begin{pmatrix} -\sin(\lambda) & \cos(\lambda) & 0 \\ -\sin(\phi)\cos(\lambda) & -\sin(\phi)\sin(\lambda) & \cos(\phi) \\ \cos(\phi)\cos(\lambda) & \cos(\phi)\sin(\lambda) & \sin(\phi) \end{pmatrix} \begin{pmatrix} v_X \\ v_Y \\ v_Z \end{pmatrix}$$

where ϕ is (geodetic) latitude and λ is longitude. Finally we project into the line of sight of the InSAR acquisition, defined locally by the unit vector (u_e,u_n,u_u):

$$v_{\mathrm{LOS}} = \begin{pmatrix} v_e \\ v_n \\ v_u \end{pmatrix} \cdot \begin{pmatrix} \hat{u}_e \\ \hat{u}_n \\ \hat{u}_u \end{pmatrix}$$

As expected, small differences between the predicted plate motion velocities exist between these two but we consider the ellipsoidal representation to be aligned with the GNSS, which also uses an ellipsoidal Earth when converting between Earth-centered Earth-fixed geocentric and local geodetic coordinates. We presented these results as part of our poster presentation at the 2022 SCEC Annual Meeting (Tymofyeyeva, Floyd, et al., 2022). Our results for each of the four tracks over Southern California currently processed and included in the CGM (InSAR) contribution, compared to the GNSS, are summarized in Figure 2.

The calculated plate correction in shown in the third (middle) row of Figure 2 for the four tracks. It resembles closely the "orbital ramp" that was commonly estimated and removed in the past when processing InSAR data and this exercise may confirm, at least partly, in addition to genuine inaccuracy in historically reported orbit data, the origin of that well known artifact. The velocity gradient induced is of the order of 1 mm/100 km and, in certain acquisition geometries, such as the ascending tracks here, is closely aligned with the deformation over the region.

The direct comparison with the CGM GNSS velocities (relative to North America) projected into InSAR line of sight, without correction of the InSAR for plate motion, is shown in the fourth row of Figure 2. The agreement between the two CGM products is approximately 2–4 mm RMS in the line of sight and the offset, described above, is clearly visible as a deviation from the one-to-one ratio marked with a diagonal dotted line. This misfit between the InSAR and GNSS is significantly improved in at least ascending track 64 and descending track 173, although ascending track 166 and descending track 71 remain much the same after correction.

We recommend that the plate motion be an explicit correction when aligning and comparing InSAR and GNSS products, even if they are pinned to the same reference point, due to the velocity gradient induced across the InSAR scene(s).

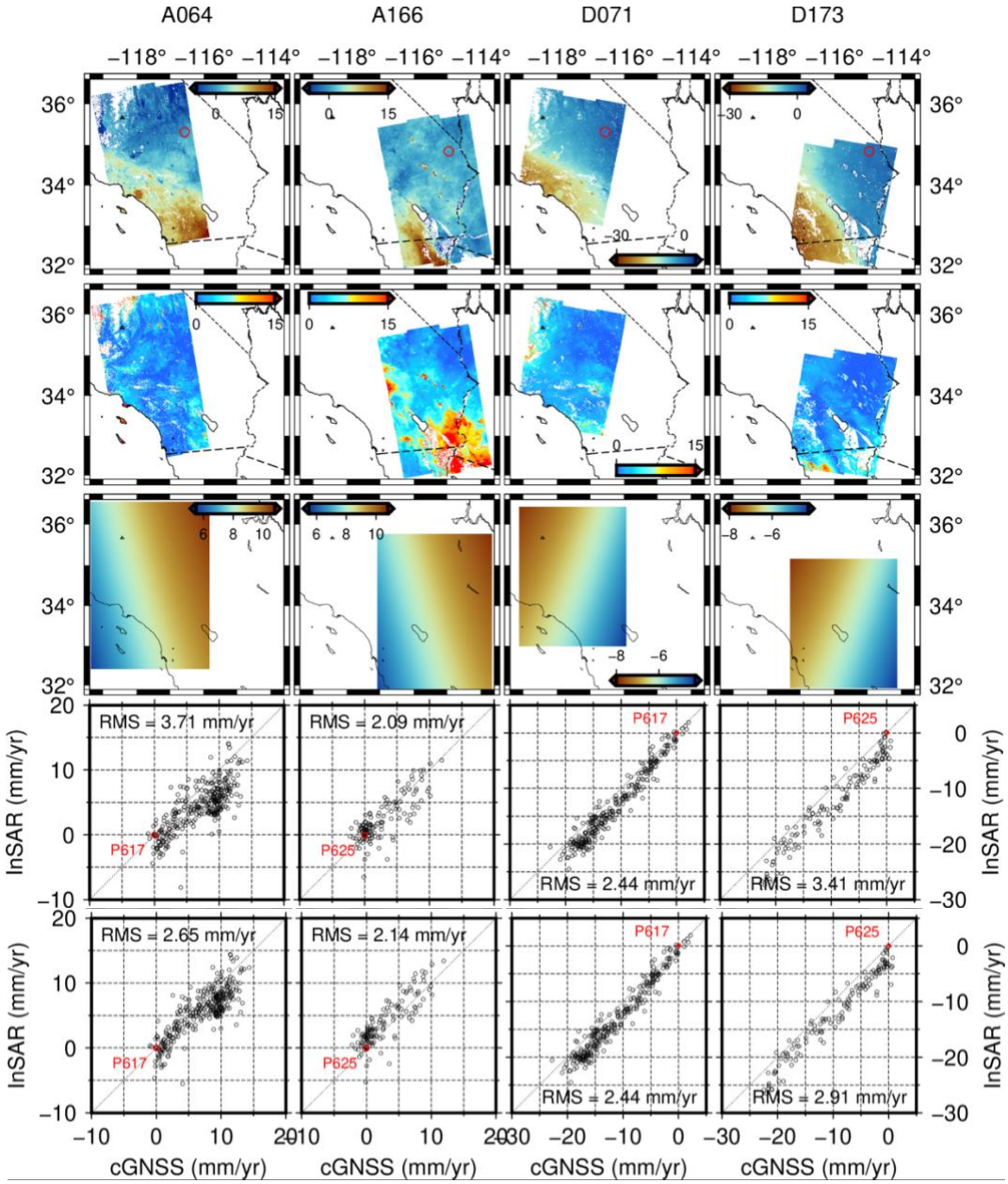

Figure 2 *Comparison of InSAR line-of-sight velocities, relative to each track's reference pixel, corresponding to the continuous GNSS station marked with a red circle (top row), and CGM GNSS velocities projected into the same line of sight over the four tracks covering Southern California. The top row shows the (original) line-of-sight velocities and the second row shows the associated uncertainties. The third row shows the calculated line-of-sight velocity change due to motion of the North America plate relative to the ITRF2014 implicit in the SAR orbit products. This correction, relative to the reference pixel, subtracted from the raw InSAR velocities is the transformation to a North America reference frame. The fourth and bottom rows compare the InSAR line-of-sight velocities with the CGM GNSS velocities projected into the line of sight before and after plate motion correction, respectively.*

Publications and products

Tymofyeyeva, E., Floyd, M., Materna, K., Funning, G. J., Liu, Z., Guns, K. A., Xu, X., Wang, K., Sangha, S. S., & Fielding, E. J. (2022, 09). Updates and improvements of the consensus InSAR Community Geodetic Model. Poster Presentation at 2022 SCEC Annual Meeting.

References

Bos, M. S., Fernandes, R. M. S., Williams, S. D. P., and Bastos, L. (2013). Fast Error Analysis of Continuous GNSS Observations with Missing Data. *Journal of Geodesy*, 87(4), 351–360. https://doi.org/10.1007/s00190-012-0605-0

Floyd, M. A., and Herring, T. A. (2020). Fast Statistical Approaches to Geodetic Time Series Analysis. In: Montillet, J.-P., and Bos, M. (eds) Geodetic Time Series Analysis in Earth Sciences. Springer Geophysics. Springer, Cham. https://doi.org/10.1007/978-3-030-21718-1_5

Stephenson, O. L., Liu, Y.-K., Yunjun, Z., Simons, M., Rosen, P., and Xu, X. (2022). The impact of plate motions on long-wavelength InSAR-derived velocity fields. *Geophysical Research Letters*, 49, e2022GL099835. https://doi.org/10.1029/2022GL099835

Williams, S. (2003). The effect of coloured noise on the uncertainties of rates estimated from geodetic time series. *Journal of Geodesy*, 76, 483–494. https://doi.org/10.1007/s00190-002-0283-4

Zhang, J., Bock, Y., Johnson, H., Fang, P., Williams, S., Genrich, J., Wdowinski, S., and Behr, J. (1997). Southern California permanent GPS geodetic array: Error analysis of daily position estimates and site velocities. *Journal of Geophysical Research*, 102(B8), 18035–18055. https://doi.org/10.1029/97JB01380